Clays and Clay Minerals, Vol. 44, No. 5, 665–671, 1996.

PARTICLE SHAPE VERSUS COHERENT SCATTERING DOMAIN OF ILLITE/SMECTITE: EVIDENCE FROM HRTEM OF DOLNÁ VES CLAYS

VLADIMÍR ŠUCHA,[1] JAN ŚRODOŃ,[2] FRANCOISE ELSASS[3] AND WILLIAM J. MCHARDY[4]

[1] Department of Geology of Mineral Deposits, Comenius University, Mlynská dolina G, 842-15 Bratislava, Slovakia

[2] Institute of Geological Sciences PAN, Senacka 1, 31-002 Kraków, Poland

[3] Station de Science du Sol INRA, Route de St-Cyr, 78000 Versailles, France

[4] The Macaulay Land Use Research Institute, Craigiebuckler, Aberdeen AB92QJ, UK

Abstract—Fundamental particle thickness measurements of Dolná Ves hydrothermal illite/smectite (I/S) samples confirmed earlier findings regarding the content of fixed cations in illite interlayers (ca. $0.9/O_{10}(OH)_2$). The distributions of fundamental particles and mixed-layer crystals of a given sample are internally consistent. In samples dominated by bilayer fundamental particles, mixed-layer crystals most often contain even numbers of layers. The expandabilities measured by XRD are much higher than so-called minimum expandabilities obtained from HRTEM measurements. This discrepancy is explained by assuming that the coherent scattering domains of Dolná Ves clays do not correspond to natural mixed-layer crystals but are thicker, probably due to parallel association of crystals on the oriented XRD slide. This tendency to produce intercrystal contacts is probably related to the unusually large *ab* dimensions of crystals of Dolná Ves clays.

Key Words—Coherent scattering domain, Fundamental particle, HRTEM, Illite/Smectite, Mixed-layer crystal.

INTRODUCTION

Mixed-layer clay minerals have generally been distinguished from mixtures of the corresponding clay minerals by X-ray diffraction (XRD) techniques. A mixed-layer clay produces an irrational series of diffraction peaks, occupying intermediate positions with respect to the corresponding peaks of the pure components according to the Mering rule. The XRD models explain this effect by assuming that the coherent scattering domain of a mixed-layer clay is composed of 2 or more types of strictly parallel layers, arranged according to different patterns. Early high resolution transmission electron microscopy (HRTEM) observations seem to confirm that assumption (Yoshida 1973). The authors of the interparticle diffraction hypothesis (Nadeau et al. 1985) challenged this opinion by suggesting that only so called "fundamental particles," that is, monolayers or sets of permanently bound (non-expanding) layers such as illite or chlorite, exist in rocks, and that the mixed-layer crystals are artifacts of the parallel aggregation of fundamental particles on the XRD slide. Later observations performed directly on undisturbed natural rocks using different techniques, such as ultramicrotomy, ion milling, and others, suggested that mixed-layer crystals occurred naturally within the rocks and that the fundamental particles observed by transmission electron microscopy (TEM) are artifacts produced by the infinite osmotic swelling of the mixed-layer crystals (Ahn and Buseck 1990; Środoń et al. 1990; Veblen et al. 1990). Reynolds (1992) has drawn the same conclusion from an XRD study of specimens of undisturbed bentonite rocks. Środoń et al. (1990) were able to measure the percentage of smectite layers in the mixed-layer crystals observed by HRTEM and found good agreement with the values measured by XRD with the implication that the mixed-layer crystals observable in natural rocks are quite stable during standard clay separation procedures for XRD. These findings are tested in the present paper using a set of hydrothermal I/S samples coming from one hydrothermal deposit (Dolná Ves, Slovakia). An attempt is also made to explain why the percentages of smectite layers in the Dolná Ves clays are significantly higher for given K content than typical values reported for I/S (Šucha et al. 1992, Figure 8).

MATERIALS AND METHODS

The samples came from the Dolná Ves hydrothermal I/S clay deposit, situated south west of the Kremnica Mts., in the Western Carpathians, Slovakia. The geology of the clay deposits in this region is presented by Kraus et al. (1979), crystallochemical aspects of the alteration products are discussed by Číčel et al. (1992) and Madejová et al. (1992). The I/S deposit was first described by Kraus et al. (1982) and later, Šucha et al. (1992) published detailed mineralogical and chemical characteristics of the I/S minerals.

Seven samples representing the full range of X-ray expandabilities known from the deposit (45 to 8%) were selected for TEM and HRTEM studies. The bulk samples were treated with $NaC_2H_3O_2$ buffer and with $Na_2S_2O_4$ (Jackson 1975) and subsequently the <1 μm fraction of Na-saturated clay was separated by sedi-

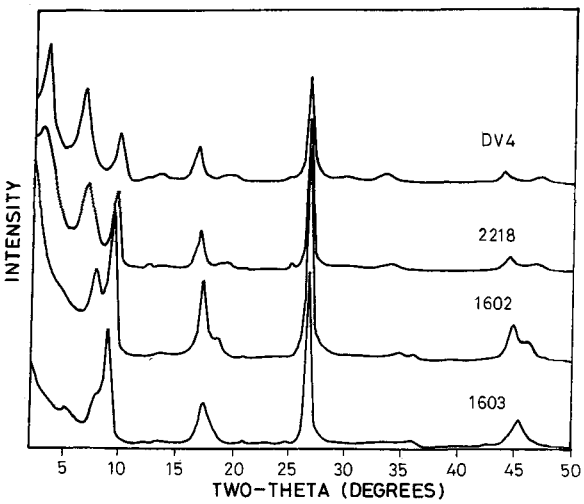

Figure 1. XRD patterns of samples illustrating the range of expandabilities of Dolná Ves clays ethylene glycol saturated.

mentation and excess soluble salts removed by dialysis. Samples were not ground but dispersed in an ultrasonic bath for 6 min prior to $NaC_2H_3O_2$ treatment.

The XRD of oriented specimens (air-dried and saturated with ethylene glycol) was carried out using a Siemens D 500 diffractometer (Ni filtered Cu-Kα radiation, graphite monochromator) at the U.S. Geological Survey in Boulder, CO. Expandabilities were determined according to the method described by Środoń and Eberl (1984). Si, Al, Mg, Ca and Fe were analyzed by spark emission spectroscopy, and Na and K were analyzed by flame spectrometry at the Centre de Géochimie de la Surface in Strasbourg. A more detailed description of the XRD and chemical analysis of the deposit is given by Šucha et al. (1992).

The TEM measurements were performed on <1 μm samples using a Siemens 102 electron microscope at the Macaulay Land Use Research Institute in Aberdeen. Fundamental particle thicknesses were measured by the Pt-shadowing technique described by Nadeau and Tait (1987) and modified by Środoń et al. (1992).

The HRTEM measurements were performed using a Philips 420 STEM microscope operated at 120 kV at the INRA laboratory in Versailles. For these investigations, 2 sample types were prepared. Small portions of <1 μm clay fractions and undisturbed rock chips were coated with agar before applying the embedding procedure described by Tessier (1984). Samples were equilibrated with pure H_2O at a pressure of 32 kPa. The H_2O was then replaced by methanol and propylene oxide. Samples were subsequently impregnated with Spurr resin. Ultrathin sections, 50 nm thick, were cut with a diamond knife on a Reichert Ultracut E microtome. During the embedding procedure, the swelling smectite interlayers were intercalated by organic components of the resin and (001) was maintained at ca. 1.35 nm (Środoń et al. 1990), whereas collapsed layers of the illite type display 1.0 nm spacings. The porosity existing between loose fundamental particles or individual mixed-layer crystals is preserved. Only the crystals having layers strictly parallel to the microscope axis display the images of the layer sequence. Pictures were taken in underfocus conditions close to the Scherzer defocus and the use of an objective aperture eliminated lattice fringes smaller than 0.35 nm. Such 1-dimensional lattice fringes can be interpreted as representations of lattice images in which variations in stacking periodicities of crystals can be examined (Iijima and Buseck 1978). The numbers of layers in individual crystals and crystal thicknesses were measured, as described in detail by Środoń et al. (1990), on photographs taken at the magnification of 51,000. Measurements were made using a binocular at a magnification between 10 and 40 times.

Table 1. Fundamental particle dimensions measured by TEM. All data are in nm.

Sample	Thickness	Length	Width	L/W	r	n
DV4	2,1	342	147	3,1	126	120
2838	2,4					107
2218	2,6	417	193	2,7	160	95
1555	2,7	347	182	2,3	142	142
1602	3,8					84
1603	4,1	438	151	3,5	145	141

Key: L/W = length/width ratio, r = mean equivalent radius of particles in a,b plane; and n = number of measured particles.

OBSERVATIONS

The distributions of fundamental particle dimensions (length, width and thickness) as measured by the Pt-shadowing method are given in Table 1 and Figure 2. No relationships between particle length, width and XRD expandability ($\%S_{XRD}$) were observed (XRD patterns of 4 samples are in Figure 1). However, mean particle thickness does increase with decreasing $\%S_{XRD}$ and the maximum frequency of particle thickness is 2 nm in 4 of the samples with the highest expandability. Two samples with a lower amount of expandable layers have maxima at 4 nm (Figure 3).

HRTEM measurements (Figure 4) of 4 clay fractions and corresponding rock chips provided information concerning the number of layers in the mixed-layer crystals (Figure 5) and there are marked differences in the distributions among samples studied by this method. The samples with the highest expandabilities 1617 (Figure 4A) and 2218 have very similar distributions. The histograms of both separated clay fractions and undisturbed rock chips have local maxima at even numbers. The relative frequency of crystallites with odd numbers of 2:1 layers significantly increase in sample 1555 but maxima at even values

https://doi.org/10.1346/CCMN.1996.0440509 Published online by Cambridge University Press

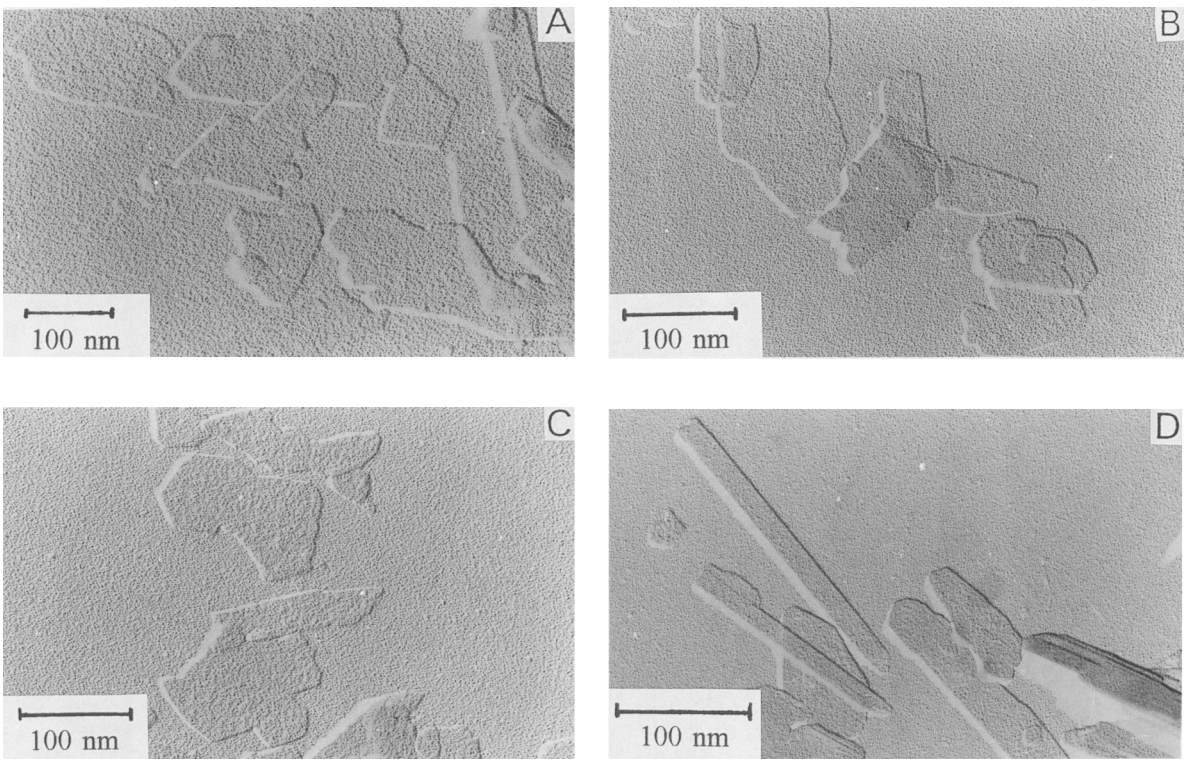

Figure 2. TEM Pt-shadowing images. A-DV4, B-2218, C-1555, D-1603.

are still present in the histogram of the specimen prepared from the bulk rock. Measurements of the <1 μm fraction of this sample show a smooth distribution of crystal thickness with continuously decreasing frequencies (Figure 5). The sample with the lowest expandability (1603, Figure 4B) also has this kind of distribution both in the clay fraction and in the bulk rock.

Expandability Calculation from HRTEM and TEM Data

Expandabilities (maximum: $\%S_{TEM}$ and $\%S_{HRTEM}$, and minimum: $\%S_{MIN}$) were calculated from TEM and HRTEM measurements according to the method described by Środoń et al. (1990, 1992). The technique of Środoń et al. (1990) assuming 1.35 nm average spacing of expandable layers was felt to be directly applicable without any modifications, because the samples were processed and imaged using exactly the same conditions and in the same laboratory. Figure 4 presents examples of HRTEM images and specifies how the mixed-layer crystals were measured. Maximum expandability ($\%S_{FIX}$) was also calculated from the fixed cation content (Table 2, data from Šucha et al. 1992) by equation $\%S_{FIX} = 95.42 - 106.76FIX$ (Środoń et al. 1992). All the data together with XRD expandabilities ($\%S_{XRD}$) from Šucha et al. (1992) are summarized in Table 2. Maximum expandabilities $\%S_{FIX}$, $\%S_{TEM}$ and $\%S_{HRTEM}$ are similar for each sample, but significant differences were observed between $\%S_{MIN}$ and $\%S_{XRD}$ in samples 1617, 2218 and 1555. Only sample 1603 has similar $\%S_{MIN}$ and $\%S_{XRD}$ values.

The relationship between expandability measured by XRD and maximum expandability ($\%S_{TEM}$) is demonstrated on the plot by Środoń et al. (1992, Figure 10). The data obtained for Dolná Ves samples do not follow the published relationship but for $\%S_{XRD} >$ 20% they follow a different line with $\%S_{XRD}$ always higher for given %SMAX (Figure 6).

The plot $\%S_{TEM}$ versus fixed cations obtained for Dolná Ves samples fits well with the line described by equation $\%S_{MAX} = 100 - 100FIX/0.9$ (Figure 7) published by Środoń et al. (1992) for I/S minerals. Two trends were found when fixed cations were plotted against $\%S_{XRD}$ (Figure 8). One trend exists for I/S minerals described by Środoń et al. (1992) and a different trend for Dolná Ves I/S minerals (Figure 5). Dolná Ves data show higher $\%S_{XRD}$ for a given content of fixed cations in expandability intervals between 25 and 45%.

DISCUSSION & CONCLUSIONS

Table 2 and Figure 8 show very good agreement obtained by 3 independent techniques of $\%S_{MAX}$ measurement—Pt-shadowing, HRTEM and the calculation

https://doi.org/10.1346/CCMN.1996.0440509 Published online by Cambridge University Press

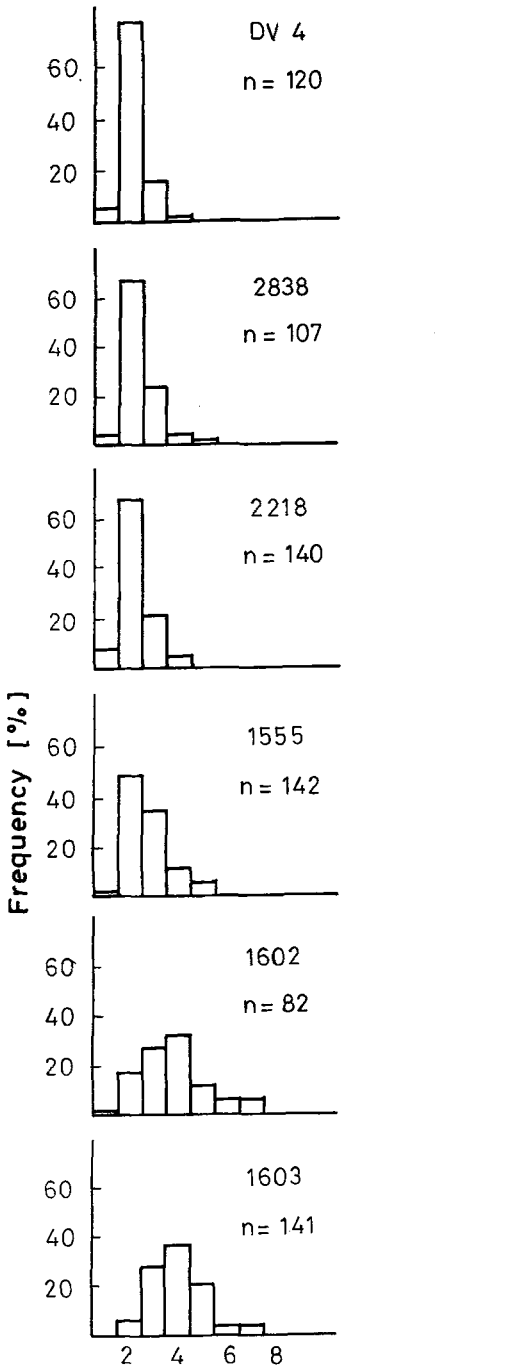

Figure 3. Histograms of fundamental particle thickness measured by TEM (Pt-shadowing method). n—number of measurements.

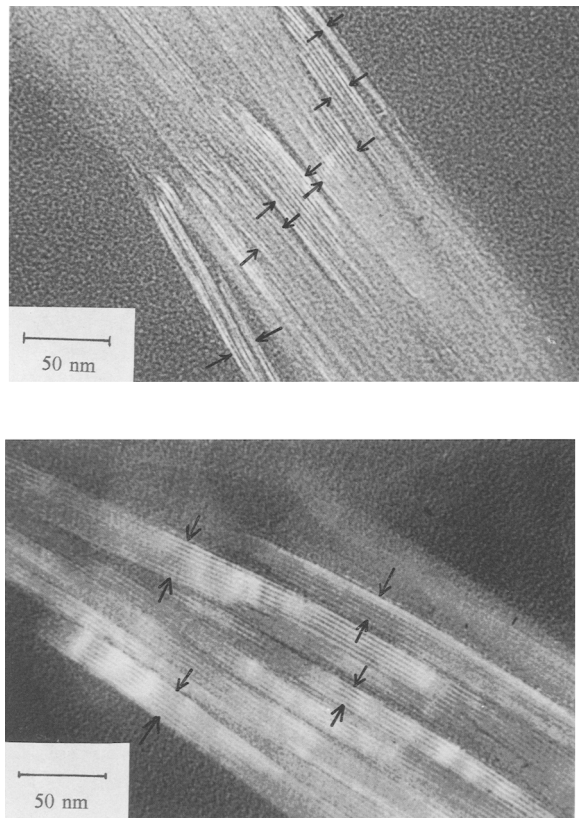

Figure 4. HRTEM images of the most smectitic -1617 and the most illitic -1603 samples studied by HRTEM. Measured cross sections of mixed-layer crystals are marked with arrows.

from fixed cations content. These measurements provide additional evidence in support of the conclusions drawn by Środoń et al. (1992) and they demonstrate that the applied TEM and HRTEM techniques of measuring mean particle thickness are precise and reproducible.

The histograms of frequencies of thickness of particles (Figure 3, TEM measurements) and the mixed-layer crystals (Figure 5, HRTEM measurements) are internally consistent: the samples dominated by 2 nm fundamental particles (bilayers) display local maxima of crystal thickness distributions at even numbers of layers, highest probability to find n × 2 layers in the mixed-layer crystals. With decreasing %S, the distributions of fundamental particles become more spread, a maximum frequency becoming less dominant and correspondingly, local even maxima less pronounced. Mean thickness of crystals is always bigger than mean thickness of fundamental particles. With decreasing expandability, the 2 values converge, as expected (Środoń et al. 1992, eq. 9). All these observations hold for the mixed-layer crystals measured in the bulk rocks and in the <1 μm fraction (Figure 5). Both measurements produced very similar histograms. The only major differences are a general shift toward thinner crystals and a big increase of % bilayers in <1 μm fraction of sample 1617. They probably result either from split-

https://doi.org/10.1346/CCMN.1996.0440509 Published online by Cambridge University Press

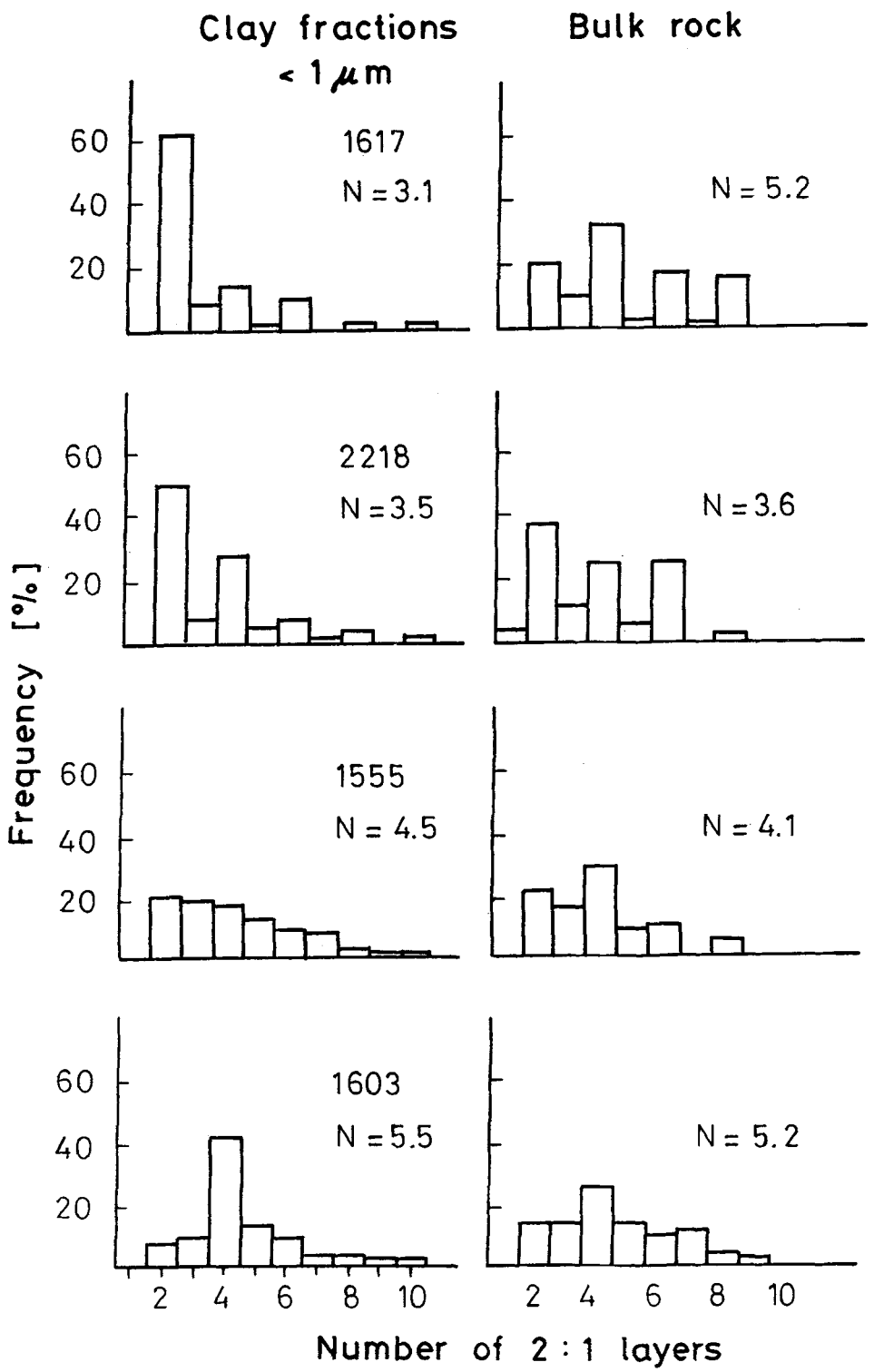

Figure 5. Histograms of numbers of 2:1 layers in the mixed-layer crystals measured by HRTEM in clay fractions and in the bulk rocks. N is the mean number of layers in a sample.

https://doi.org/10.1346/CCMN.1996.0440509 Published online by Cambridge University Press

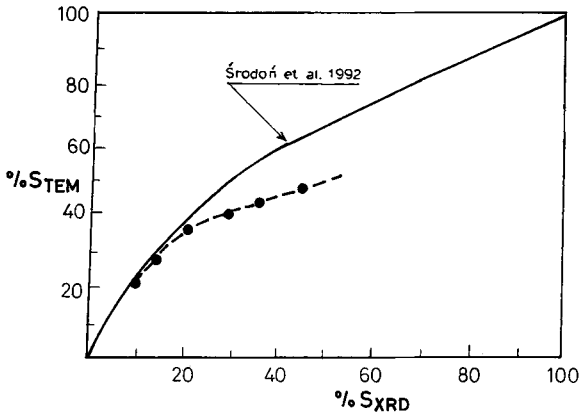

Figure 6. Relation between $\%S_{TEM}$ and $\%S_{XRD}$. Solid line is from Środoń et al. (1992).

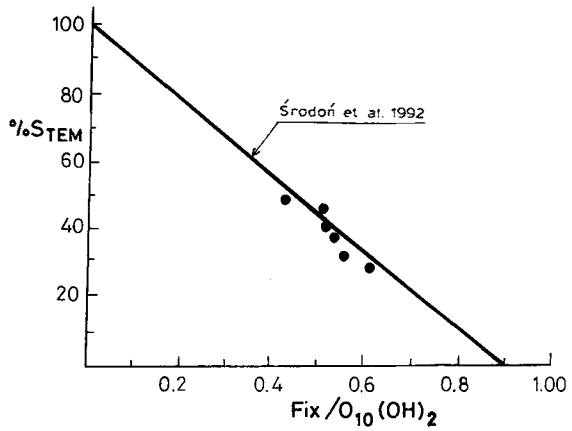

Figure 7. Relation between $\%S_{TEM}$ and the content of fixed cations/$O_{10}(OH)_2$. Solid line is from Środoń et al. (1992).

ting of mixed-layer crystals or from fractionation in the course of the separation process. Środoń et al. (1990) made similar observation on a sample of similar expandability.

Figures 6 and 8 document the same phenomenon using 2 independent sets of data (TEM and chemical composition); the more smectitic samples from Dolná Ves are characterized by substantially higher $\%S_{XRD}$ for a given maximum expandability (or fixed cations content) than the values measured for bentonites by Środoń et al. (1992). For the most smectitic sample (DV4) $\%S_{MAX}$ and $\%S_{XRD}$ are almost identical. This is interpreted to mean that the coherent scattering domains are so thick that the short stack effect (Eberl and Środoń 1988) is almost eliminated. This conclusion does not correspond to the measurements of mixed-layer crystal thickness of both clay fractions and rock chips done by HRTEM, where the average numbers of layers per crystal are 3 to 5, so they are even smaller than the 5 to 7 range reported by Środoń et al. (1990) for bentonites of comparable expandability. Correspondingly, calculated minimum expandabilities ($\%S_{MIN}$) are smaller than $\%S_{XRD}$. It is also in contradiction with Środoń et al. (1990) who reported very close agreement between the 2 measurements. The only explanation for these observations is that the coherent scattering domains of Dolná Ves clays do not correspond to the mixed-layer crystals observed by HRTEM, but they are thicker. A tentative conclusion is that the Dolná Ves crystals produce an "intercrystal diffraction effect" resulting from their high ability to build face-to-face contacts in the course of preparation of the oriented specimens for XRD. It may be that the large *a, b* dimensions of the Dolná Ves clays (equivalent radius of 120 to 160 nm as opposed to 40 to 90 nm reported by Środoń et al. (1992) for bentonites of the same expandability range) together with the high flexibility of these thin particles are responsible for their unusual behavior. The closest $\%S_{MIN}$ and $\%S_{XRD}$ values were obtained for sample 1603. In this sample, the mean thickness of fundamental particles is highest (Table 1), so the particles are more rigid and produce less face-to-face contacts.

An opposite phenomenon, lower $\%S_{XRD}$ for given $\%S_{MAX}$, described by Środoń and Elsass (1994), was

Table 2. Expandability calculations for studied samples based on TEM, HRTEM, XRD and chemical data.

	XRD data	TEM data		HRTEM data							Chemical data	
				Bulk rock				Clay fraction				
Sample	$\%S_{XRD}$	$\%S_{TEM}$	n	$\%S_{HRTEM}$	$\%S_{MIN}$	N	n	$\%S_{HRTEM}$	$\%S_{MIN}$	N	Fix	$\%S_{FIX}$
DV4	45	48									0,43	49
1617	40		100	36	21	5,2	90	43	15	3,1	0,46	46
2838	36	42									0,51	41
2218	29	38	127	36	11	3,6	108	40	16	3,5	0,48	44
1555	21	37	158	31	9	4,1	174	34	16	4,5	0,52	40
1602	14	26									0,56	35
1603	8	24	106	27	10	5,2	77	24	3	5,5	0,61	30

Key: $\%S_{XRD}$ = expandability measured by XRD; $\%S_{TEM}$ = maximum expandability calculated from electron microscopy data (Pt-shadowing technique); n = number of measured particles; $\%S_{HRTEM}$ = maximum expandability calculated from HRTEM data; $\%S_{MIN}$ = minimum expandability calculated from HRTEM data; N = mean number of layers in mixed layer crystals; Fix = content of fixed cations per half unit cell; and $\%S_{FIX}$ = maximum expandability calculated from Fix.

https://doi.org/10.1346/CCMN.1996.0440509 Published online by Cambridge University Press

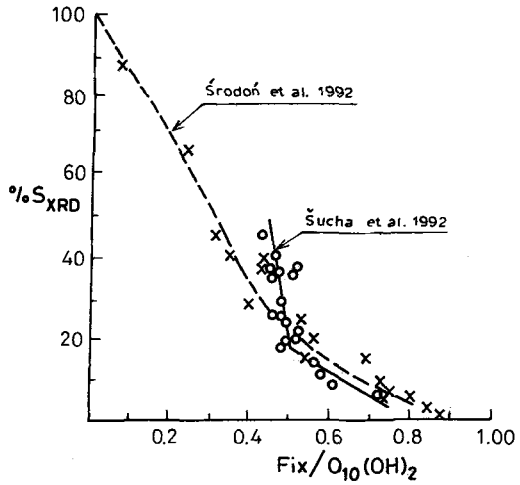

Figure 8. Relation between $\%S_{XRD}$ and the content of fixed cations. Crosses represent data of Środoń et al. (1992), circles are data from this study.

also explained as a result of particle shape. Combining both effects, it is conceivable that by using the plot of $\%S_{MAX}$ versus $\%S_{XRD}$ and the line representing "normal" illite/smectites (Środoń et al. 1992) it should be possible to recognize "anomalous" shapes of particles without electron microscopy. Note that $\%S_{MAX}$ can be calculated from fixed cations content or from the mean particle thickness measured by XRD. Significantly elevated $\%S_{XRD}$ for given $\%S_{MAX}$ should indicate extremely large, flexible particles, whereas, significantly lower $\%S_{XRD}$ for given $\%S_{MAX}$ could be due to the extremely elongated (filamentous illite) or barrel shaped particles.

ACKNOWLEDGMENTS

Thanks to V. Drits and D. R. Peacor for helpful comments. V. Šucha and J. Środoń thank la Direction des Relations Internationales de INRA (France) for supporting their visits to Versailles. V. Šucha also acknowledges the financial support from the US-Slovak Science and Technology Program, project 92029 and the Slovak Grant Agency (Grant 1/1809/94).

REFERENCES

Ahn JH, Buseck PR. 1990. Layer-stacking techniques and structural disorder in mixed-layer illite/smectite: Image simulation and HRTEM imaging. Am Mineral 75:267–275.

Číčel B, Komadel P, Bednáriková E, Madejová J. 1992. Mineralogical composition and distribution of Si, Al, Fe, Mg and Ca in the fine fraction of some Czech and Slovak bentonites. Geol Carpath-Series Clays 43:3–7.

Eberl DD, Środoń J. 1988. Ostwald ripening and interparticle diffraction effects for illite crystals. Am Mineral 73:1335–1345.

Iijima S, Buseck PR. 1978. Experimental study of disordered mica structures by high-resolution electron microscopy. Acta Crystall 34:709–719.

Jackson ML. 1975. Soil chemical analysis—Advanced course. Madison, WI: Published by the author. 389 p.

Kraus I, Šamajová E, Zuberec J. 1979. Mineral composition of altered products of rhyolite volcanism at the SW margin of the Kremnické pohorie Mts. In: Konta J, editor. Proceedings of the 8th Conf. Clay Miner. Petrol. in Teplice, Carol Pragensis: Geol. Univ. p 137–144.

Kraus I, Číčel B, Šamajová E, Machajdík D. 1982. Origin and genesis of the clays resulting from alteration of rhyolite volcanic rocks in Central Slovakia. Geol Z Geol Carpath 33:269–275.

Madejová J, Komadel P, Číčel B. 1992. Infrared spectra of some Czech and Slovak smectites and their correlation with structural formulas. Geol Carpath-Series Clays 43:9–12.

Nadeau PH, Wilson MJ, McHardy WJ, Tait JM. 1985. The conversion of smectite to illite during diagenesis: Evidence from some illitic clays from bentonites and sandstones. Mineral Mag 49:393–400.

Nadeau PH, Tait JM. 1987. Transmission electron microscopy. In: Wilson MJ, editor. A handbook of determinative methods in clay mineralogy. London: Blackie. p 209–247.

Reynolds RC. 1992. X-ray diffraction studies of illite/smectite from rocks, <1 μm randomly oriented powders, and <1 μm oriented powder aggregates: The absence of laboratory-induced artifacts. Clays Clay Miner 40:387–396.

Środoń J, Eberl DD. 1984. Illite. In: Micas, Mineralogical Society of America Reviews in Mineralogy 13:495–544.

Środoń J, Andreolli C, Elsass F, Robert M. 1990. Direct high-resolution transmission electron microscopic measurement of expandability of mixed-layer illite/smectite in bentonite rocks. Clays Clay Miner 38:373–379.

Środoń J, Elsass F, McHardy WJ, Morgan DJ. 1992. Chemistry of illite-smectite inferred from TEM measurements of fundamental particles. Clay Miner 27:137–158.

Środoń J, Elsass F. 1994. Effect of the shape of fundamental particles on XRD characteristics of illitic minerals. Eur J Mineral 6:113–122.

Šucha V, Kraus I, Mosser CH, Hroncová Z, Soboleva KA, Širáňová V. 1992. Mixed-layer illite/smectite from the Dolná Ves hydrothermal deposit, The Western Carpathians, Kremnica Mts. Geol Carpath-Series Clays 43:13–19.

Tessier D. 1984. Étude experimental de l'organisation des materiaux argileux [Dr. Science thesis]. Univ. Paris VII: Paris, INRA publisher. 361 p.

Veblen DR, Guthrie GD, Livi KJT, Reynolds RC, Jr. 1990. High-resolution transmission electron microscopy and electron diffraction of mixed-layer illite/smectite: Experimental results. Clays Clay Miner 38:1–13.

Yoshida T. 1973. Elementary layers in the interstratified clay minerals as revealed by electron microscopy. Clays Clay Miner 21:413–420.

(Received 20 December 1994; accepted 3 January 1996; Ms. 2601)